

This is the accepted manuscript of the article that appeared in final form in *Journal of Inorganic Biochemistry* 181 : 111-116 (2017), which has been published in final form at <https://doi.org/10.1016/j.jinorgbio.2017.10.014>. © 2017 Published by Elsevier Inc under CC BY-NC-ND license (<http://creativecommons.org/licenses/by-nc-nd/4.0/>)

Aluminum's preferential binding site in proteins: sidechain of amino acids versus backbone interactions.

Jon I. Mujika¹, Gabriele Dalla Torre¹, Elena Formoso¹, Rafael Grande-Aztatzi¹, Slawomir J. Grabowski^{1,2}, Christopher Exley³ and Xabier Lopez^{1,*}

- 1) Kimika Fakultatea, Euskal Herriko Unibertsitatea UPV/EHU, and Donostia International Physics Center (DIPC), P.K. 1072, 20080 Donostia, Euskadi, Spain.
- 2) IKERBASQUE, Basque Foundation for Science 48011 Bilbao (Spain)
- 3) Birchall Centre, Lennard-Jones Laboratories, Keele University, Staffordshire, ST5 5BG, UK

The interaction of aluminum ion Al(III) with polypeptides is a subject of paramount importance, since it is a central feature to understand its deleterious effects in biological systems. Various drastic effects have been attributed to aluminum in its interaction with polypeptides and proteins. These interactions are thought to be established mainly through the binding of aluminum to phosphorylated and non-phosphorylated amino acid sidechains. However, a new structural paradigm has recently been proposed, in which aluminum interacts directly with the backbone of the proteins, provoking drastic changes in their secondary structure and leading ultimately to their denaturation. In the present paper, we use computational methods to discuss the possibility of aluminum to interact with the backbone of peptides and compare it with the known ability of aluminum to interact with amino acid sidechains. To do so, we compare the thermodynamics of formation of prototype aluminum-backbone structures with prototype aluminum-sidechain structures, and compare these results with previous data generated in our group in which aluminum interacts with various types of polypeptides and known aluminum biochelators. Our results clearly points to a preference of aluminum towards amino acid sidechains, rather than towards the peptide backbone. Thus, structures in which aluminum is interacting with the carbonyl group are only slightly exothermic, and they become even less favorable if the interaction implies additionally the peptide nitrogen. However, structures in which aluminum is interacting with negatively-charged sidechains like aspartic acid, or phosphorylated serines are highly favored thermodynamically.

KEYWORDS: Aluminum specificity, Binding energy, DFT, QTAIM

1. Introduction

During the last century, the massive introduction of aluminum in daily life has dramatically increased its bioavailability, altering the natural geochemical cycle that has consistently maintained the most abundant metal element in the Earth's crust absent from biota.[1] Unfortunately, the burden of aluminum we suffer is likely to have deep consequences, still not fully understood at the molecular level. Aluminum has been demonstrated to be involved in diseases such as dialysis encephalopathy,[2] and this element is nowadays accepted as a risk factor in neurodegenerative diseases,[3] such as Alzheimer disease (AD).

Due to its chemical properties, aluminum ion Al(III) has the capability of interacting with many biological molecules, which makes the mapping of these interactions difficult. Moreover, the complexes formed by aluminum with different biological building blocks are highly dependent on factors such as pH, concentration, *etc...* Therefore, the study of the interaction of biological molecules with aluminum (refer to aluminum speciation) is still challenging and presents inherent difficulties using experimental techniques alone. In this sense, theoretical methods have become a fundamental tool to characterize the structure and thermodynamics of aluminum compounds with biological molecules.[4]

As a hard Lewis acid, aluminum shows preference towards oxygen donor ligands, such as carboxylates, phosphates, nucleotides (NADH, ATP,...) and nucleic acids such as DNA.[5,6] Similarly, polypeptides and proteins are a clear target of this cation and in fact aluminum has been proven to inhibit the activity of several proteins, mainly because of a strong interaction with a phosphate cofactor.[7,8] Aluminum may also contribute in the development of AD by promoting the formation and growing of the two most clear hallmarks in the disease[9–12]: i) intracellular neurofibrillary tangles (NFT) composed of hyperphosphorylated tau protein and ii) A β fibrils, the main constituent in senile plaques, which are mainly made of aggregated A β peptides.

More recently, Song *et al.*,[13] have suggested a new paradigm in the type of aluminum-protein interaction. They have proposed aluminum could directly interact

with the backbone of the proteins, forming very stable structures with a characteristic 5-member ring, in which aluminum is directly coordinated to the carbonyl oxygen and a deprotonated peptide nitrogen, forming strong covalent bonds. This type of binding motif would lead to a dramatic change on the secondary structure of the protein, altering its conformation and provoking its denaturation. However, the existence of this type of binding motif is difficult to reconcile with previous experimental[12,14] and theoretical studies[15,16] that have unequivocally established the propensity of aluminum to interact with amino acid sidechains with Al-O bonds of mainly electrostatic nature.

In the present paper, we apply different quantum methods to determine the thermodynamics of aluminum binding to the backbone of proteins. To do so, we consider a series of model structures based on the work of Song *et al.*,[13] and we compare their binding energies to model structures in which aluminum is interacting with the sidechain of an amino acid. We also compare our results with previous calculations of model polypeptides in which the interaction is mediated through a variety of sidechains, including phosphorylated serines, known biological low-molecular-mass (LMM) chelators such as citrate, and a variety of phosphate molecules. Our results clearly point to a preference of aluminum to interact with amino acid sidechains, with backbone structures much less favorable thermodynamically.

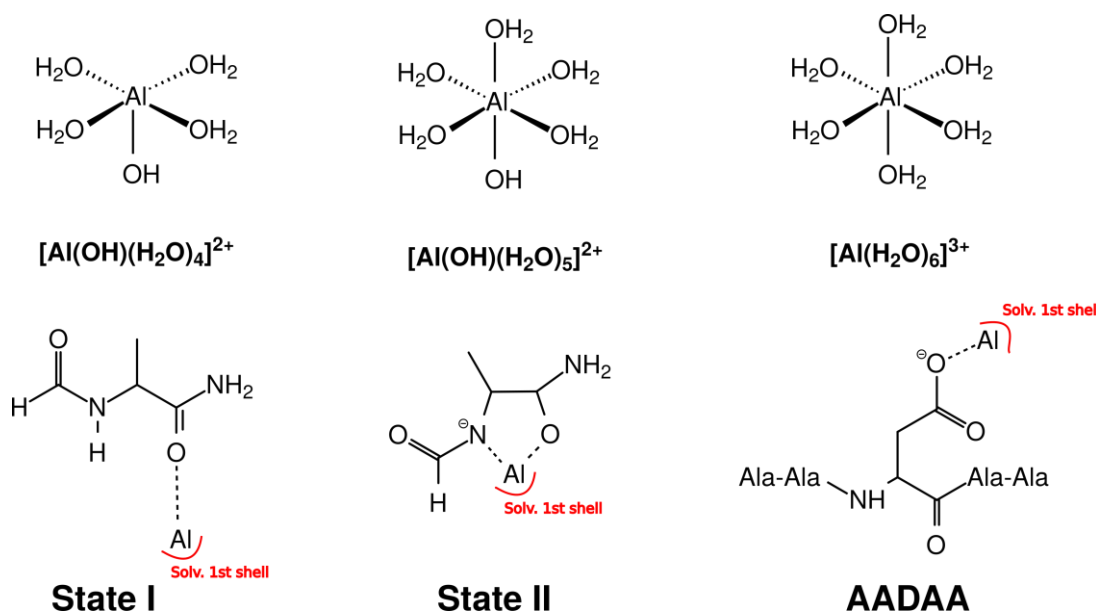


Figure 1: Schematic representation of the structures characterized.

2. Methodology

Al(III) can form a large variety of different hydrated species.[17] Herein three hydrated Al(III) structures were considered (see Figure 1): i) Al(III) interacting with a hydroxide and four water molecules ($[\text{Al}(\text{OH})(\text{H}_2\text{O})_4]^{2+}$), ii) Al(III) interacting with a hydroxide and five water molecules ($[\text{Al}(\text{OH})(\text{H}_2\text{O})_5]^{2+}$) and iii) Al(III) interacting with six water molecules ($[\text{Al}(\text{H}_2\text{O})_6]^{3+}$). Moreover, two Al(III)-peptide structures were optimized (see Figure 1): i) Al(III) interacts with the peptide bond carbonyl oxygen (referred to as State I) and ii) Al(III) interacts with the peptide bond carbonyl oxygen and the deprotonated N atom (referred to as State II). For these two structures, the coordination shell of Al(III) was fulfilled based on the three coordination shells considered for the hydrated Al(III), that is: i) pentacoordinated with one hydroxide in the coordination shell (as in ref [13], no subscript added) ii) pentacoordinated and shell completed with water molecules (the “1,5” subscript added) and iii) hexacoordinated and shell completed with water molecules (the “0,6” subscript added). All the structures are represented in Figure 1 and the optimized geometries illustrated in Figure 2.

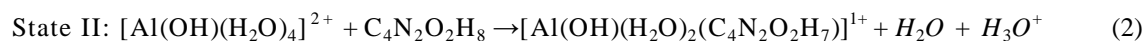
All geometrical optimizations were carried out in aqueous phase using the Gaussian 09 program,[18] B3LYP functional[19–21] and 6-31++G(d,p) basis set. To confirm that optimized structures were real minima on the potential energy surfaces, frequency calculations were carried out at the same level of theory. All structures showed positive force constants for all normal modes of vibration. The frequencies were then used to evaluate the zero-point vibrational energy (ZPVE) and thermal (T=298 K) vibrational corrections to the Gibbs free energies within the harmonic oscillator approximation. To calculate the entropy, the different contributions to the partition function were evaluated using the standard statistical mechanics expressions in the canonical ensemble and the harmonic oscillator and rigid rotor approximation. The solvent effect was introduced using the self-consistent reaction field (SCRF) method with the polarized continuum model (PCM), using the integral equation formalism variant (IEFPCM).[22]

The electronic energies were refined by single-point energy calculations at the B3LYP/6-311++G(3df,2p) level of theory, both in gas-phase and in solution, and then used to estimate energies in gas-phase (E_{gas}) and in solution (E_{aq}). On the other hand, the free energy contributions computed by the frequency calculations were added to E_{aq} to determine the free energy in solution (G_{aq}). Moreover, single-point calculations at the MP2/6-311++G(3df,2p) level of theory were carried out both in the gas-phase and in aqueous environment in order to assess the accuracy of the results. In spite of some deviations between the relative energies computed with the B3LYP functional and MP2, in all cases the trends observed with the DFT functional are corroborated by the MP2 method, and for the sake of simplicity only the DFT results will be discussed in the body text.

3. Results

3.1 Interaction with the backbone of proteins

As a first approach, we follow the proposal of Song *et al.*, [13] who employed a small model to analyze the interaction between Al(III) and the backbone of a peptide (an alanine capped by H atoms, shown in Figure 1), with the reference structure for Al(III) in solution taken as a pentacoordinate $[\text{Al}(\text{OH})(\text{H}_2\text{O})_4]^{2+}$. Based on this model, they characterized two Al(III)-peptide structures (illustrated in Figures 1 and 2 and referred to as State I and II in their paper and hereafter). In State I, Al(III) interacts with the peptide bond carbonyl oxygen, while in State II, both the carbonyl oxygen and the deprotonated peptide nitrogen interact with Al(III), forming a five-member ring. They evaluated the binding energies (ΔE) of State I and II according to the following reactions:



Their results pointed to a high stabilization of both States I and State II with ΔE values of -27.05 kcal/mol and -50.71 kcal/mol at the MP2 level of theory. Due to the high stability of State II, the authors concluded that Al(III) can indeed form five-member rings with the backbone of proteins. Furthermore, based on the analysis of orbitals and

Mulliken charges the authors suggested a significant reduction of aluminum in State II, with a significant covalent nature of the bond between aluminum and the carbonyl oxygen and peptide nitrogen. This capacity of aluminum to form chemical bonds with the backbone of proteins would lead naturally to the formation of highly stable five-member ring structures with their backbone, provoking their denaturalization, and being an important molecular mechanism to understand aluminum toxicity.

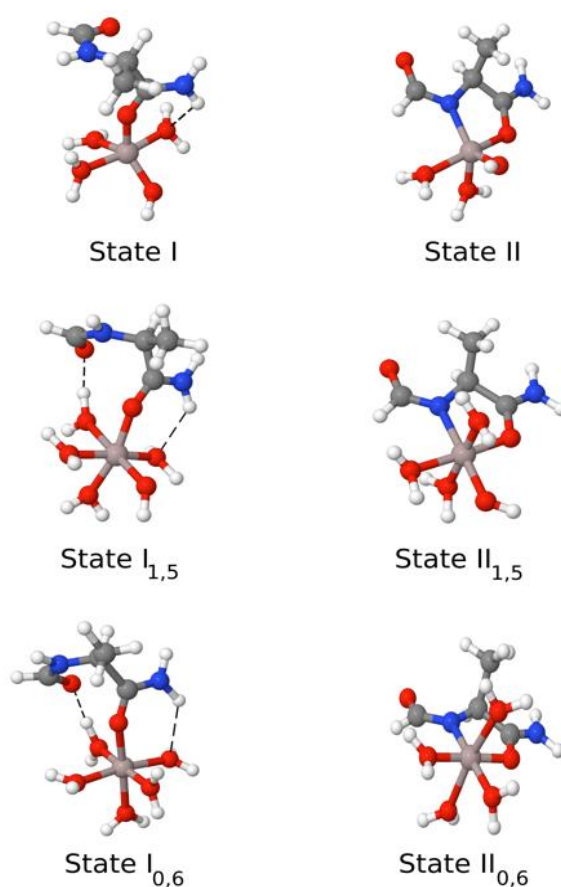


Figure 2: State I corresponds to the binding of aluminum to the peptide bond carbonyl oxygen, whereas State II corresponds to the formation of an Al-N bond from State I. Both structures characterized considering three different coordination shells for Al(III) (nomenclature defined in Methodology section). Atoms represented as: O (red), H (white), C (grey) and N (blue).

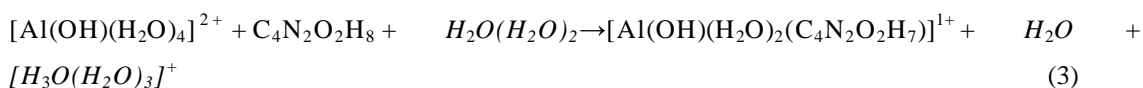
However, these results were obtained based on binding energies computed in the gas-phase, and therefore a proper treatment of bulk solvent effects is needed to account for the possibility of the formation of these structures in a biological aqueous environment. On the other hand, the authors took as a reference in aqueous environment a

pentacoordinated $[\text{Al}(\text{OH})(\text{H}_2\text{O})_4]^{2+}$ species.[13] However, both experiments[23,24] and computational studies[17] indicate that Al(III) shows preference towards being octahedral in aqueous solution, either coordinated to six water molecules, i.e. $[\text{Al}(\text{H}_2\text{O})_6]^{3+}$, or with a combination of one hydroxide and five water molecules, $[\text{Al}(\text{OH})(\text{H}_2\text{O})_5]^{2+}$. [17]

Table 1: Thermodynamics of Formation of State I and II. Reaction energies and free energies computed at different level of theories: a) MP2, taken from ref [13]; b) MP2/6-311++G(3df,2p) in the gas-phase; c) MP2/6-311++G(3df,2p) in aqueous environment using the IEFPCM continuum model; d) B3LYP/6-311++G(3df,2p) in the gas-phase; e) B3LYP/6-311++G(3df,2p) in aqueous environment using the IEFPCM continuum model. Three different structure of hydrated aluminum are taken as reference for these two reactions: $[\text{Al}(\text{OH})(\text{H}_2\text{O})_4]^{2+}$, $[\text{Al}(\text{OH})(\text{H}_2\text{O})_5]^{2+}$ or $[\text{Al}(\text{H}_2\text{O})_6]^{3+}$. For each state, the superscript corresponds to the label of the reaction used to calculate the energy of the corresponding compound.

	MP2			DFT		
	$\Delta E_{\text{gas}}^{(a)}$	$\Delta E_{\text{gas}}^{(b)}$	$\Delta E_{\text{aq}}^{(c)}$	$\Delta E_{\text{gas}}^{(d)}$	$\Delta E_{\text{aq}}^{(e)}$	$\Delta G_{\text{aq}}^{(e)}$
$[\text{Al}(\text{OH})(\text{H}_2\text{O})_4]^{2+}$						
<i>State I⁽¹⁾</i>	-27.1	-40.2	-13.0	-38.9	-11.1	-7.6
<i>State II⁽²⁾</i>	-50.7	-44.9	17.2	-41.9	20.7	13.2
<i>State II⁽³⁾</i>	-	-112.6	-14.4	-110.5	-11.8	-8.0
$[\text{Al}(\text{OH})(\text{H}_2\text{O})_5]^{2+}$						
<i>State I⁽¹⁾</i>	-	-41.6	-13.6	-39.5	-10.7	-2.9
<i>State II⁽²⁾</i>	-	-33.1	26.3	-29.0	30.7	25.0
<i>State II⁽³⁾</i>	-	-100.9	-5.4	-97.7	-1.8	3.7
$[\text{Al}(\text{H}_2\text{O})_6]^{3+}$						
<i>State I⁽¹⁾</i>	-	-70.7	-17.1	-69.4	-14.7	-11.1
<i>State II⁽²⁾</i>	-	-130.9	20.4	-127.9	24.0	20.7
<i>State II⁽³⁾</i>	-	-198.7	-11.3	-196.6	-8.6	-0.6

Therefore, we decided to calculate the binding/formation energies for State I and II introducing *i*) bulk solvent effects through the use of a continuum model in the context of DFT level of theory, *ii*) entropic effects by evaluating binding free energies (ΔG) and *iii*) using additionally, more reliable hydrated aluminum structures as reference so that three coordination shells are chosen: $[\text{Al}(\text{OH})(\text{H}_2\text{O})_4]^{2+}$ (used in ref [13]), $[\text{Al}(\text{OH})(\text{H}_2\text{O})_5]^{2+}$, and $[\text{Al}(\text{H}_2\text{O})_6]^{3+}$. In addition, we would like to note that dealing with a small charged molecule such as a hydronium ion involves some technical difficulties, mainly an accurate estimation of its solvation energy. In order to alleviate this shortcoming, the microsolvated hydronium model ($\text{H}_3\text{O}(\text{H}_2\text{O})_3$) and its neutral counterpart were used to calculate the energy of State II:



Results are summarized in Table 1 and all geometries characterized illustrated in Figure 2. We start comparing the results of State I and II according to reaction (1) and (2), that is, using the bare hydronium to evaluate the energies of State II. For gas phase calculations and taking the $[\text{Al}(\text{OH})(\text{H}_2\text{O})_4]^{2+}$ species as reference, we obtain similar gas phase energies as ref [13] for State I and II, -38.9 kcal/mol and -41.9 kcal/mol, respectively. However, the introduction of solvent effects has a profound effect on the thermodynamics of these charged systems, and now although formation of State I is still exothermic, -11.1 kcal/mol, State II is highly endothermic, 20.7 kcal/mol, and therefore unlikely to be formed in aqueous solution. The change of hydrated aluminum reference structure to $[\text{Al}(\text{OH})(\text{H}_2\text{O})_5]^{2+}$ or $[\text{Al}(\text{H}_2\text{O})_6]^{3+}$ has a sizeable effect on the gas phase energetic and especially for the case of $[\text{Al}(\text{H}_2\text{O})_6]^{3+}$, with a significant increase in the gas-phase exothermicities for the formation of States I and II. However, again the introduction of solvent effects yields an increase in the ΔE_{aq} values, with the result that only the formation of State I is moderately exothermic, while formation of State II is highly endothermic in all cases. Similarly, the computed ΔG_{aq} values confirm this trend, with values of State II between 13.2 to 25 kcal/mol depending on the hydrated aluminum structure taken as reference. Note that this is somehow expected, since State II requires the deprotonation of a peptide bond nitrogen, and this is a very unfavorable process in solution according to the high values of the pK_a 's of amides.

Interestingly, the relative energies of State II decreases in ca. 20 kcal/mol (see Table 1) when its binding energies are evaluated using the microsolvated $\text{H}_3\text{O}(\text{H}_2\text{O})_3$ model (reaction 3) instead of the bare hydronium ion, and consequently the difference between the energies of State I and State II shrinks. In spite of this modification, State II remains clearly less stable than State I when Al(III) presents any of the two octahedral arrangement, and only with Al(III) pentacoordinated the stability of the two compounds are similar. However, as pointed out above, this coordination mode is the most unlikely one for Al(III). More importantly, all these results confirm on one hand that special cautions should be taken evaluating binding energies and choosing the reference molecule, and on the other hand that the interaction of Al(III) with the backbone of a peptide bond (either State I or II) can not compete with the interaction of the cation with a negatively charged side chain (see below).

Song *et al.*[13] claimed that the energy required to deprotonate the peptide bond N atom could be somehow compensated by a strong binding of the carbonyl oxygen and peptide nitrogen to aluminum, with a significant degree of covalent character, and significant reduction of the aluminum oxidation state. Their analysis was based on the analysis of orbitals shapes and Mulliken charges, which shows inherent limitations.[25] We decided to analyze the bonding features of State I and II generated by the $[\text{Al}(\text{OH})(\text{H}_2\text{O})_4]^{2+}$ structure using the more accurate Quantum Theory of Atoms in Molecules (QTAIM).[26] Briefly, the theory makes use of an unambiguous partition of electron density in atom basins based on Bader's definition of an atom in a molecule (zero-flux condition). In this context, the bonding between two atoms is characterized by the so-called bond critical point (BCP). Various properties at the BCP's characterize the type of bonding, in particular the value of the density (ρ_{BCP}), the laplacian of the density ($\nabla^2 \rho_{\text{BCP}}$), and the energy density (H_{BCP}) are commonly used to classify the type of bonding (covalent versus ionic) between a pair of atoms. In Table 2, we summarize the values obtained for all the Al-O and Al-N bonds found in State I and State II. Typical covalent bonds show negative values of both the laplacian and the energy density at the BCP. This indicates that the accumulation of the electronic charge at BCP leads to stabilization of the bonding interaction. On the contrary, ionic bonds show typically positive values of the laplacian and the energy density.[27] As one can see in Table 2, all Al-O bonds of State I fall into the latter category. The formation of State II does not change the qualitative picture for Al-O bonds, whereas in the case of Al-N

bond, we find also a positive value of the laplacian, and only a very small negative value of the energy density at the bond critical point. This can be related to very minor dative interactions from the nitrogen lone pair into the empty valence shell of aluminum, but not to a strong chemical bond due to the reduction of the aluminum oxidation state. In fact, the Bader atomic charges show only a very slight reduction of the charge of aluminum, from 2.578 to 2.546 a.u., when passing from State I to State II, another evidence of the mainly electrostatic nature of the bonding interactions between the peptide atoms and aluminum. Analogous results were obtained for the State I and II structures with Al(III) hexacoordinated.

Table 2: QTAIM analysis of Al-O and Al-N bonding. Values of the electron density (ρ_{BCP}), laplacian of electron density ($\nabla^2\rho_{\text{BCP}}$) and energy density (H_{BCP}) at the bond critical point for all Al-X (X=O,N) bonds in States I and II structures characterized considering the [1,5] and [0,6] coordination shells (defined in the Methodology section). All quantities in atomic units.

	ρ_{BCP}	$\nabla^2\rho_{\text{BCP}}$	H_{BCP}		ρ_{BCP}	$\nabla^2\rho_{\text{BCP}}$	H_{BCP}
State I_{1,5} ($Q_{\text{Al}} = +2.578$ a.u.)				State II_{1,5} ($Q_{\text{Al}} = +2.546$ a.u.)			
Al-O ^{carb}	0.073	0.573	0.010	Al-N	0.076	0.449	-0.005
Al-O ^{OH}	0.097	0.832	0.008	Al-O ^{carb}	0.060	0.392	0.004
Al-O ^{W1}	0.050	0.331	0.005	Al-O ^{OH}	0.093	0.787	0.008
Al-O ^{W2}	0.059	0.427	0.009	Al-O ^{W1}	0.052	0.359	0.007
Al-O ^{W3}	0.049	0.320	0.005	Al-O ^{W2}	0.045	0.281	0.004
State I_{0,6} ($Q_{\text{Al}} = +2.604$ a.u.)				State II_{0,6} ($Q_{\text{Al}} = +2.572$ a.u.)			
Al-O ^{carb}	0.066	0.498	0.008	Al-N	0.075	0.426	-0.006
Al-O ^{W1}	0.062	0.439	0.007	Al-O ^{carb}	0.067	0.459	0.004
Al-O ^{W2}	0.051	0.333	0.005	Al-O ^{W1}	0.051	0.328	0.005
Al-O ^{W3}	0.054	0.358	0.005	Al-O ^{W2}	0.048	0.300	0.004
Al-O ^{W4}	0.055	0.381	0.006	Al-O ^{W3}	0.047	0.295	0.004
Al-O ^{W5}	0.053	0.352	0.005	Al-O ^{W4}	0.052	0.347	0.005

3.2 Interaction with amino acid sidechains

In summary, the calculations carried out in the model employed in ref [13] do not support the idea of a strong interaction of Al(III) with the peptide backbone through the formation of 5-member rings (State II) in aqueous solution, although the interaction with the carbonyl oxygen (State I) could still be favorable thermodynamically. However, taking into account that the bond between aluminum and the carbonyl oxygen or nitrogen is mainly of electrostatic character, one could think that it could not compete with the interaction with other functional groups commonly present in residues, such as negatively charged carboxylic groups (Asp/Glu sidechains or C-terminals in proteins). In fact, it is well known that Al(III) has large affinity towards negatively charged carboxylic or phosphates groups.[28] To analyze this point, we evaluate the binding interaction energy of aluminum to a carboxylic sidechain in Ala-Ala-Asp-Ala-Ala (AADAA) pentapeptide (See Figures 1 and 3). Results (shown in Table 3) clearly show a much larger exothermicity for the resultant structure with values of -48.7 kcal/mol.

In addition, we also provide in Table 3, the thermodynamics of relevant structures found in our previous works, with similar quantum methods. For instance, in the case of the experimentally and theoretically studied GEGEGSGG octapeptide we obtain different ΔG values depending on the coordination of aluminum.[15] We have chosen three paradigmatic cases: i) N1-GEGEGSGG where aluminum interacts with only one aspartate sidechain, -33.7 kcal/mol, N6-GEGEGSGG which shows one aspartate sidechain in the first coordination shell and a second carboxylate group in the second coordination sphere, -67.9 kcal/mol, and finally, P1-GEGEGSGG with a phosphorylated serine coordinating aluminum, -78.2 kcal/mol. All cases show a more favorable interaction than with the models in which aluminum is directly interacting with the peptide backbone. It is remarkable the enhancement of affinity obtained upon phosphorylation of the serine sidechain and increase in the negative charge associated to the corresponding residue. Notice as well, the tendency of aluminum to favor structures in which several functional groups coordinate aluminum, (either in the first coordination sphere or in the second one). In this sense, the most favorable interaction is obtained for A β peptide,[16] where three carboxylic groups (Glu3, Asp7 and Glu11) bind to aluminum in the first coordination shell. Thus, the simultaneous interaction with various negatively charged groups present in the A β peptide sequence makes this polypeptide to be highly favorable for aluminum binding.[29]

The conclusion of our data is clear: in the aqueous phase, it is thermodynamically more favorable for Al(III) to interact with negative charged amino acid sidechains rather than with the backbone of proteins. Even with just one negatively charged amino acid sidechain, there is a substantial strengthening of the binding to aluminum with respect to only backbone interactions.

Are these sidechain interactions of sufficient strength as to be relevant in biological systems? To answer this question we need to compare our data with that obtained with similar methods for known low molecular mass biochelators of aluminum. In Table 3, we displays the thermodynamics of aluminum chelation by citrate, the main LMM chelator in blood serum, and by relevant biophosphates such as 2,3-DPG, glucose-6-phosphate (G6P), NADH, and ATP-like triphosphates (TriP). The order in binding energies is the following one: citrate (-124.9) > 2,3-DPG (-123.5) \approx G6P (-117.2) > TriP (-108.7) \gg NADH (-54.0 kcal/mol). It is clear that based on these results and among the Al-peptide interactions shown in this work, only the Al-A β complex could be considered as a competitive strong chelator in biological systems. Therefore, a high density of negative charged amino acid sidechains in a reduced sequence region seems to be a prerequisite for a polypeptide to have a high affinity for aluminum.

Table 3: Thermodynamics of the binding to Al(III) of i) peptide through its backbone (State I and II compounds) and ii) other relevant biological molecules. Reaction energies calculated according to equations (1) and (2) (taking $[\text{Al}(\text{H}_2\text{O})_6]^{3+}$ as reference state), computed at B3LYP/6-311++G(3df,2p) with IEFPCM continuum model to include solvent effects.

Ligand	Ref.	Ligand Charge	Binding Mode	ΔH_{aq}	ΔG_{aq}
Interaction with the backbone					
<i>State I</i> _{0,6}	This work	0	Backbone O(C)	-14.7	-11.1
<i>State II</i> _{0,6}	This work	-1	Backbone N&O(C)	24.0/-8.6	20.7/-0.6
Interaction with the sidechain of aminoacids					
AADAA	This work	-1	Asp	-	-48.7
GEGEGSGG	[15]	-2	N1	-36.5	-33.7
			N6	-69.7	-67.9
GEGEGS(P)GG	[15]	-4	P1	-81.0	-78.2
A β ₁₋₁₆ peptide	[16]	-2	Glu3,Asp7,Glu11	-172.9 ⁽¹⁾	-
Interaction with LMM Ligands					
Citrate	[30,31]	-4	2 COO ⁻ ,O ⁻	-133.0	-124.9
2,3-DPG	[31]	-5	Multiple	-118.9	-123.5
NADH	[32]	-1	Multiple	-	-54.0
Glucose-6-Phosphate	[33]	-3	Multiple	-116.5	-117.2
ATP-like, Triphosphate	[34]	-4	α,β -Phosphate	-109.2	-108.7

(1) ΔE_{aq} value

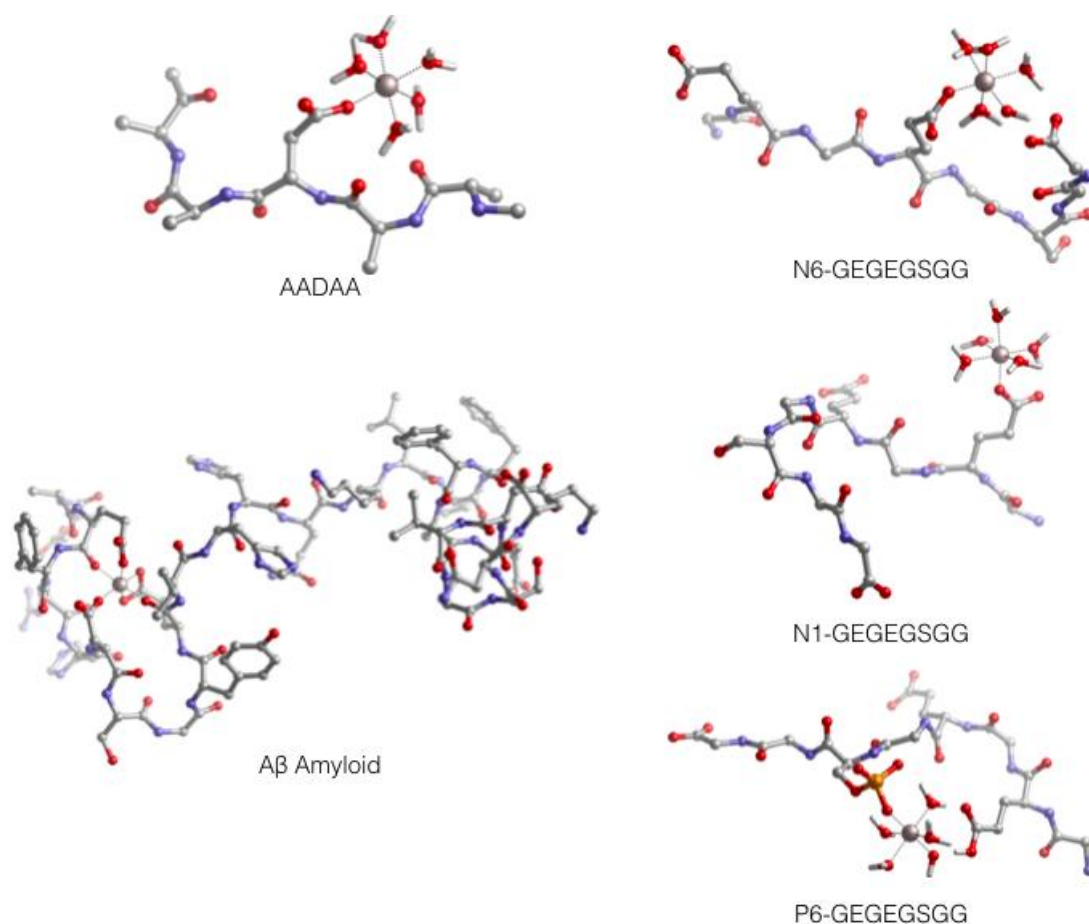


Figure 3: Structures of different polypeptide structures considered in Table 3. Note that for clarity hydrogen atoms are not displayed.

4 Conclusions

In this paper, we have revised the possibility of aluminum to interact with the backbone of proteins, using density functional theory in conjunction with continuum solvation models to treat bulk solvent effects. To do so, we have compared the thermodynamics of formation of Al(III)-backbone structures previously proposed in the literature, with those structures in which aluminum interacts with amino acid sidechains, and with known aluminum low molecular mass chelators in biological systems. We have found that in an aqueous environment aluminum shows a clear preference to interact with negatively charged amino acid sidechains, with aluminum-backbone structures being much less favorable thermodynamically than aluminum-sidechain structures. The comparison with known biochelators of aluminum, like citrate or biophosphates, clearly indicates that only in cases in which there is a high density of negatively charged amino acid sidechains in proteins, such as in A β peptide, could a biomolecule be a competitive aluminum chelator in biological environments.

Table of Abbreviations

DFT: Density Functional Theory.

B3LYP: Becke, three-parameter, Lee-Yang-Parr DFT functional.

MP2: Møller–Plesset perturbation theory.

Ab: Amyloid beta peptide.

IEFPCM: Integral equation formalism of polarizable continuum model.

ATP: Adenosine triphosphate.

NADH: Nicotinamide adenine dinucleotide.

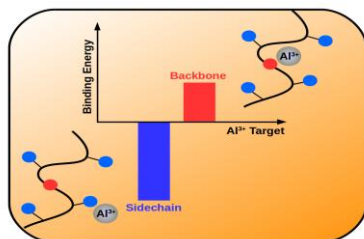
Acknowledgements

Technical and human support was provided by SGI/IZO (SGIker) of UPV/EHU and European funding (ERDF and ESF). Financial support comes from UPV/EHU (PES14/35), Eusko Jaurlaritza (IT588-13) and the Spanish Ministerio de Ciencia e Innovación (MINECO/FEDER) (CTQ2015-67608-P).

References:

- [1] C. Exley, A biogeochemical cycle for aluminium?, *J. Inorg. Biochem.* 97 (2003) 1–7.
- [2] A.C. Alfrey, G.R. LeGendre, W.D. Kaehny, The Dialysis Encephalopathy Syndrome: Possible Aluminum Intoxication, *N. Engl. J. Med.* 294 (1976) 184–188.
- [3] C. Exley, Aluminum Should Now Be Considered a Primary Etiological Factor in Alzheimer's Disease, *J. Alzheimer's Dis. Rep.* 1 (2017) 23–25.
- [4] J.I. Mujika, E. Rezabal, J.M. Mercero, F. Ruipérez, D. Costa, J.M. Ugalde, X. Lopez, Aluminium in biological environments: A computational approach, *Comput. Struct. Biotechnol. J.* 9 (2014) e201403002.
- [5] T.L. Macdonald, R. Bruce Martin, Aluminum ion in biological systems, *Trends Biochem. Sci.* 13 (1988) 15–19.
- [6] M. Nicolini, P.F. Zatta, B. Corain, Aluminium in Chemistry, Biology and Medicine, in: *Life Chem. Rep.*, 1994: pp. 3–98.
- [7] J.C.K. Lai, J.P. Blass, Inhibition of Brain Glycolysis by Aluminum, *J. Neurochem.* 42 (1984) 438–446.
- [8] J.M. Socorro, R. Olmo, C. Teijón, M.D. Blanco, J.M. Teijón, Analysis of aluminum-yeast hexokinase interaction: modifications on protein structure and functionality, *J. Protein Chem.* 19 (2000) 199–208.
- [9] S. Bhattacharjee, Y. Zhao, J.M. Hill, M.E. Percy, W.J. Lukiw, Aluminum and its potential contribution to Alzheimer's disease (AD), *Front. Aging Neurosci.* 6 (2014) 2013–2015.
- [10] M. Kawahara, M. Kato-Negishi, Link between Aluminum and the Pathogenesis of Alzheimer's Disease: The Integration of the Aluminum and Amyloid Cascade Hypotheses., *Int. J. Alzheimers Dis.* 2011 (2011) 276393.
- [11] L. Tomljenovic, Aluminum and Alzheimer's disease: after a century of controversy, is there a plausible link?, *J. Alzheimers Dis. JAD.* 23 (2011) 567–598.
- [12] C. Exley, The coordination chemistry of aluminium in neurodegenerative disease, *Coord Chem Rev.* 256 (2012) 2142–2146.
- [13] B. Song, Q. Sun, H. Li, B. Ge, J.S. Pan, A.T.S. Wee, Y. Zhang, S. Huang, R. Zhou, X. Gao, F. Huang, H. Fang, Irreversible denaturation of proteins through aluminum-induced formation of backbone ring structures, *Angew Chem Int Ed.* 53 (2014) 6358–6363.
- [14] T. Kiss, From coordination chemistry to biological chemistry of aluminium, *J. Inorg. Biochem.* 128 (2013) 156–163.
- [15] R. Grande-Aztatzi, E. Formoso, J.I. Mujika, J.M. Ugalde, X. Lopez, Phosphorylation promotes Al(III) binding to proteins: GEGEGSGG as a case study, *Phys. Chem. Chem. Phys.* 18 (2016) 7197–7207.
- [16] J.I. Mujika, J. Rodríguez-Guerra, X. Lopez, J.M. Ugalde, L. Rodríguez-Santiago, M. Sodupe, J.-D. Maréchal, Elucidating the 3D structures of Al(III)-A β complexes: a template free strategy based on the pre-organization hypothesis, *Chem Sci.* 8 (2017) 5041–5049.
- [17] W. Yang, Z. Qian, Q. Miao, Y. Wang, S. Bi, Density functional theory study of the aluminium(III) hydrolysis in aqueous solution., *Phys. Chem. Chem. Phys.* 11 (2009) 2396–401.
- [18] M.J. Frisch, G.W. Trucks, H.B. Schlegel, G.E. Scuseria, M.A. Robb, J.R. Cheeseman, G. Scalmani, V. Barone, B. Mennucci, G.A. Petersson, H. Nakatsuji, M. Caricato, X. Li, H.P. Hratchian, A.F. Izmaylov, J. Bloino, G. Zheng, J.L. Sonnenberg,

- M. Hada, M. Ehara, K. Toyota, R. Fukuda, J. Hasegawa, M. Ishida, T. Nakajima, Y. Honda, O. Kitao, H. Nakai, T. Vreven, J.A. Montgomery Jr., J.E. Peralta, F. Ogliaro, M. Bearpark, J.J. Heyd, E. Brothers, K.N. Kudin, V.N. Staroverov, R. Kobayashi, J. Normand, K. Raghavachari, A. Rendell, J.C. Burant, S.S. Iyengar, J. Tomasi, M. Cossi, N. Rega, J.M. Millam, M. Klene, J.E. Knox, J.B. Cross, V. Bakken, C. Adamo, J. Jaramillo, R. Gomperts, R.E. Stratmann, O. Yazyev, A.J. Austin, R. Cammi, C. Pomelli, J.W. Ochterski, R.L. Martin, K. Morokuma, V.G. Zakrzewski, G.A. Voth, P. Salvador, J.J. Dannenberg, S. Dapprich, A.D. Daniels, Ö. Farkas, J.B. Foresman, J.V. Ortiz, J. Cioslowski, D.J. Fox, Gaussian 09 Revision A.1, n.d.
- [19] A.D. Becke, Density-functional exchange-energy approximation with correct asymptotic-behavior, *Phys Rev A*. 38 (1988) 3098–3100.
- [20] A.D. Becke, Density-functional thermochemistry .3. The ole of exact exchange, *J Chem Phys*. 98 (1993) 5648–5652.
- [21] C. Lee, W. Yang, R.G. Parr, Development of the Colle-Salvetti correlation-energy formula into a functional of the electron density *Phys Rev B*. 37 (1988) 785–789.
- [22] J. Tomasi, B. Mennucci, R. Cammi, Quantum mechanical continuum solvation models, *Chem Rev*. (2005) 2999–3093.
- [23] G. Johansson, Structures of Complexes in Solution Derived from X-Ray Diffraction Measurements, in: *Adv. Inorg. Chem.*, Elsevier, 1992: pp. 159–232.
- [24] I. Persson, Hydrated metal ions in aqueous solution: How regular are their structures?, *Pure Appl. Chem*. 82 (2010) 1901–1917.
- [25] B. Szefczyk, W.A. Sokalski, J. Leszczynski, Optimal methods for calculation of the amount of intermolecular electron transfer, *J. Chem. Phys*. 117 (2002) 6952–6958.
- [26] R.F.W. Bader, *Atoms in Molecules, A Quantum Theory.*, Oxford University Press, Oxford, 1990.
- [27] G. Gervasio, R. Bianchi, D. Marabello, About the topological classification of the metal–metal bond, *Chem. Phys. Lett*. 387 (2004) 481–484.
- [28] R.B. Martin, The chemistry of aluminum as related to biology and medicine, *Clin. Chem*. 32 (1986) 1797–1806.
- [29] C. Exley, Price, N. C., Kelly, S. M, Birchall, J. D., An interaction of P-amyloid with aluminium in vitro, *FEBS Lett*. 324 (1993) 293–295.
- [30] J.I. Mujika, J.M. Ugalde, X. Lopez, Aluminum speciation in biological environments. The deprotonation of free and aluminum bound citrate in aqueous solution., *Phys. Chem. Chem. Phys. PCCP*. 14 (2012) 12465–12475.
- [31] N. Luque, J.I. Mujika, E. Formoso, X. Lopez, Aluminum interaction with 2,3-diphosphoglyceric acid. A computational study, *RSC Adv*. 5 (2015) 63874–63881.
- [32] E. Formoso, J.I. Mujika, S.J. Grabowski, X. Lopez, Aluminum and its effect in the equilibrium between folded/unfolded conformation of NADH, *J. Inorg. Biochem*. 152 (2015) 139–146.
- [33] E. Formoso, X. Lopez, A computational study on interaction of aluminum with D -glucose 6-phosphate for various stoichiometries, *RSC Adv*. 7 (2017) 6064–6079.
- [34] N.B. Luque, J.I. Mujika, E. Rezabal, J.M. Ugalde, X. Lopez, Mapping the affinity of aluminum(III) for biophosphates: Interaction mode and binding affinity in 1:1 complexes, *Phys. Chem. Chem. Phys*. 16 (2014) 20107–20119.



Graphical abstract

Synopsis

The binding of aluminum to a protein backbone is less favorable than its binding to negatively charged side chains

Highlights

1. Negatively charged oxygen containing amino acids are the preferential coordination site of $Al(III)$ in proteins
2. Our computational calculations confirm that the interaction of $Al(III)$ to side chains is more stable than its interaction with the protein backbone
3. Solvent effects must be introduced to obtain significant results
4. The interaction of $Al(III)$ with the peptide bond carbonyl group is thermodynamically more favorable than the formation of a 5-member ring with the carbonyl group and a deprotonated peptide nitrogen.
5. The bonds between aluminum and the backbone carbonyl oxygen or nitrogen are mainly of electrostatic character.